Jahn-Teller effect and relaxation processes in the $^1T_{2g}$ state of Ni^{2+} in MgO

N. Moreau, A. C. Boccara, and J. Badoz
Laboratoire d'Optique Physique EPCI, 10, rue Vauquelin, 75231 Paris Cedex 05, Paris*
(Received 19 October 1973)

The $^1T_{2g}$ relaxed excited state of Ni^{2+} in MgO was studied through the magnetic and stress-induced polarization of the emission spectrum. Evidence for a Jahn-Teller coupling with an E_g mode was found ($E_{JT} \sim 515$ cm^{-1}). The stress and temperature dependence of relaxation processes have been analyzed, showing the existence of a one-phonon-induced tunneling process.

I. INTRODUCTION

A number of Jahn-Teller excited states have been studied with success through optical techniques. The behavior of the zero-phonon line and of the vibronic spectrum under an external perturbation[1,2] can provide quantitative information (Ham factor and Jahn-Teller energy).

The lattice coupling of Ni^{2+} in MgO is known to be fairly strong, and evidence for a Jahn-Teller effect in the infrared $^3T_{2g}$ level has been found by Sturge through the behavior of the zero-phonon line under stress.

In the present study, we were interested in the Jahn-Teller coupling of the $^1T_{2g}$ fluorescing state. This coupling was investigated by Manson,[3] who showed, by analyzing the band shape of the emission spectrum that this level interacts mainly with E_g modes. However, Bird *et al.*[4] claimed that they could explain their dichroism measurements without assuming any Jahn-Teller effect. We have been looking, therefore, for experimental evidence and quantitative information about Jahn-Teller coupling.

The technique used by Sturge for the $^3T_{2g}$ state was not available in this case, since the $^3A_{2g} \rightarrow {}^1A_{2g}$ transition does not exhibit a zero-phonon line. Moreover, the well-resolved vibronic lines of the spectrum are too broad (100 cm^{-1}) to make a direct observation of their splitting possible. However, experimental evidence for the Jahn-Teller effect, and an estimation of its magnitude, could be obtained through the use of differential techniques in emission. In addition, in the temperature range where the fluorescence lifetime and the relaxation time have the same order of magnitude, relaxation processes could be analyzed through their temperature and stress dependence in a very simple way.

In Sec. II we will briefly describe the experimental arrangement. In Sec. III, we will review the performance of the calculation of selection rules by using detailed matrix elements which allow the proper calculation of electric dipole moments in any configuration, i.e., under any perturbation. We will analyze in Sec. IV the magnetic and stress experiments in the excited state, and discuss them, in order to deduce quantitative information. In Sec. V, the relaxation processes will be analyzed through the stress experiments, the discussion in Sec. VI being centered on the physical origin of the tunneling matrix element.

II. EXPERIMENTAL

The sample of Ni^{2+} in MgO was placed in a helium Dewar, where it was either immersed in liquid helium (1.3–4.2 K) or cooled by a flow of helium gas (5–30 K). It was optically excited at 4040 Å (transition $^3A_{2g} \rightarrow {}^3T_{1g}$) by a xenon arc through a low-resolution monochromator. The emission spectrum was detected using a second monochromator followed by a photomultiplier. We used a photoelastic modulator,[5] whose birefringence was modulated at the frequency ω, followed by a Glan-Thomson polarizer in order to analyze the circular polarization of the emission spectrum in the presence of a magnetic field, as well as the linear polarization under stress. In order to detect the degree of circular polarization (P_C), the modulator was set at $\pm \frac{1}{4}\lambda$ and the lock-in detector was operated at the frequency ω. If the degree of linear polarization (P_L) was to be detected, the modulator was made $\pm \frac{1}{2}\lambda$ and the lock-in detector was adjusted to the frequency 2ω (Fig. 1). The sensitivity of our device depends, of course, on the intensity of the fluorescence. Although the emission from the $^1T_{2g}$ state is not very strong, we could nevertheless measure, with a time constant of 14 sec, a degree of circular or linear polarization of a few 10^{-4}.

We define the degree of circular or linear polarization in the usual way;

$$P_C = (I_{\sigma_+} - I_{\sigma_-})/(I_{\sigma_+} + I_{\sigma_-}) ,$$

where I_{σ_+} and I_{σ_-} are the intensities of σ_+ and σ_- light, respectively;

$$P_L = (I_{\parallel} - I_{\perp})/(I_{\parallel} + I_{\perp}) ,$$

where $I_{\parallel}$ and $I_{\perp}$ are, respectively, the intensities of linearly polarized light parallel or perpendicular to the applied stress.

III. SELECTION RULES

The symmetry of the Ni^{2+} ion site is O_h. Thus, in the electric dipole approximation, the transition

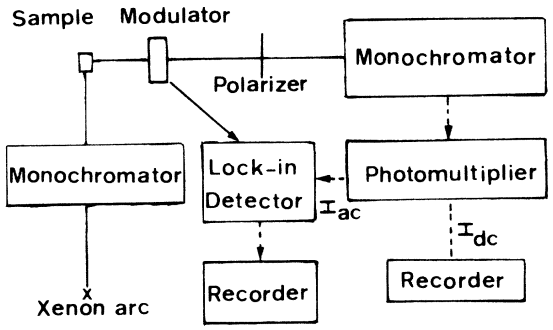

FIG. 1. Block diagram for detection of P_L and P_C.

$^1T_{2g} \rightarrow {}^3A_{2g}$ is both spin and parity forbidden.

It has already been shown[6] that the transition becomes spin allowed through second-order spin-orbit coupling between the $^1T_{2g}$ and the $^3T_{1g}$ (T_2) components, and electric dipole allowed if mixing with an excited odd configuration through odd vibrational T_{1u} modes is considered. In particular, the first two lines of the fluorescence spectrum have been assigned to one-phonon T_{1u} lines.[3] Using group theory, we have calculated the relative intensities of their linearly and circularly polarized components in various cubic wave function bases in order to interpret the behavior of the system under magnetic and stress perturbations.

This calculation requires an exhaustive transcription of the matrix element which is involved in the electric dipole transition[3]; in particular, the specification of the phonon state for each T_{1u} component is needed in the description of the vibronic states, in order to unambiguously calculate the transition probability from the relaxed excited state $|^1T_{2g}, 0, 0, 0\rangle$ (0, 0, 0 represents the vibrational wave function of the T_{1u} mode, meaning that there is no phonon in any of the T_{1u} components) to the final vibronic ground state, which may be $|^3A_{2g}, 1, 0, 0\rangle$; $|^3A_{2g}, 0, 1, 0\rangle$; or $|^3A_{2g}, 0, 0, 1\rangle_-$. This description, given by Manson, was nevertheless, not used by him to calculate selection rules, since he was mainly interested in shape functions.

Other authors have calculated the selection rules for σ_+ and σ_- lights associated with the $^1T_{2g} \rightarrow {}^3A_{2g}$ transition, the Ni^{2+} ion being in a different crystal, but still in O_h symmetry. However, they could not independently consider the transitions to the different vibronic ground states,[7] since they did not entirely specify the phonon states in vibronic wave functions.

It should be noted that, in the case of a magnetic perturbation, and of circularly polarized light, the calculation mentioned in the previous paragraph happens to lead to the right result. However, this is not the case for linearly polarized transitions, where the use of proper formulas is required to get a correct result. The selection rules thus calculated are given in Table I.

IV. JAHN-TELLER COUPLING

It has been pointed out by Ham[8] that, in the case of an orbital triplet interacting with an E_g mode, the off-diagonal matrix elements of electronic operators calculated within the vibronic ground state are reduced, the quenching factor being $Q = e^{(-3E_{JT}/2\hbar\omega)}$, where E_{JT} stands for the Jahn-Teller energy and $\hbar\omega$ is the energy of the interacting mode.

The Zeeman and the trigonal stress operators are thus expected to be reduced, whereas a tetrag-

TABLE I. Polarization and relative line intensities of the T_{1u} one-phonon-assisted $^1T_{2g} \rightarrow {}^3A_{2g}$ transition in various cubic bases.

Magnetic field $\langle 100 \rangle$	$\lvert {}^1T_{2g}, +1\rangle$	$\lvert {}^1T_{2g}, 0\rangle$	$\lvert {}^1T_{2g}, -1\rangle$
$\lvert {}^3A_{2g}\rangle$	$\sigma_-(2)$ $\sigma_+(1)$	$\sigma_-(1)$ $\sigma_+(1)$	$\sigma_-(1)$ $\sigma_+(2)$
Stress $\langle 001 \rangle$	$\lvert {}^1T_{2g}, YZ\rangle$	$\lvert {}^1T_{2g}, ZX\rangle$	$\lvert {}^1T_{2g}, XY\rangle$
$\lvert {}^3A_{2g}\rangle$	$X(2)$ $Y(1)$ $Z(1)$	$X(1)$ $Y(2)$ $Z(1)$	$X(1)$ $Y(1)$ $Z(2)$
Stress $\langle 110 \rangle$	$\lvert {}^1T_{2g}, XY\rangle$	$(1/\sqrt{2})(\lvert {}^1T_{2g}, YZ\rangle + \lvert {}^1T_{2g}, ZX\rangle)$	$(1/\sqrt{2})(\lvert {}^1T_{2g}YZ\rangle - \lvert {}^1T_{2g}ZX\rangle)$
$\lvert {}^3A_{2g}\rangle$	$110(1)$ $1\bar{1}0(1)$ $001(2)$	$110(2)$ $1\bar{1}0(1)$ $001(1)$	$1\bar{1}0(1)$ $110(2)$ $001(1)$

onal stress must give rise to an unquenched splitting.

Since we do not know the coupling coefficients of the $^1T_{2g}$ level to the stress, we cannot conclude that a possible quenching of the splitting induced by a trigonal stress exists. On the contrary, the g factor of this level may be calculated, thus making possible the comparison between theoretical and experimental magnetic splittings.

A. Magnetic measurements

The circular polarization of the emission spectrum induced by a magnetic field, like the magnetic circular dichroism, includes terms whose origin is the change in energy of the transition (the so-called diamagnetic terms), and terms which arise from the difference in population between the Zeeman sublevels. We restrict our study here to the latter terms, since they dominate in the spectra.

For an orbitally triply degenerate emitting state (assuming that Boltzman equilibrium is reached in it) the P_C expected from Table I is

$$P_C = (e^x - e^{-x})/(3e^x + 3e^{-x} + 2) ,$$

where

$$x = \delta E/kT .$$

$\delta E = g\mu_B H$ is the splitting induced by the magnetic field; μ_B is the Bohr magneton; H is the magnetic field; T is the temperature.

The orbital g factor is estimated using the parameters of Bird *et al.*[4]; taking into account second-order spin-orbit coupling with the $^3T_{1g}$ (T_2) state, it is found to be[9]

$$g = \langle {}^1T_{2g} + 1 \,|\, L_z + 2S_z \,|\, {}^1T_{2g} + 1 \rangle = 1.1 .$$

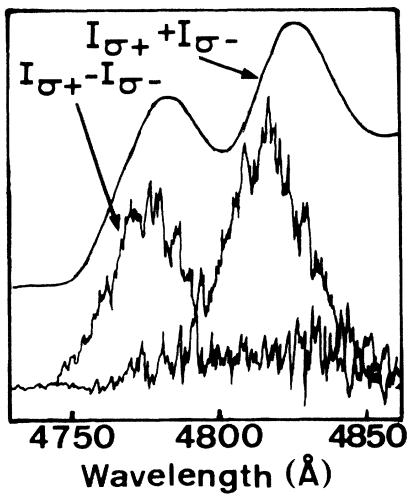

FIG. 2. P_C experimental spectrum. $T = 1.27$ K, $H = 0.85T$.

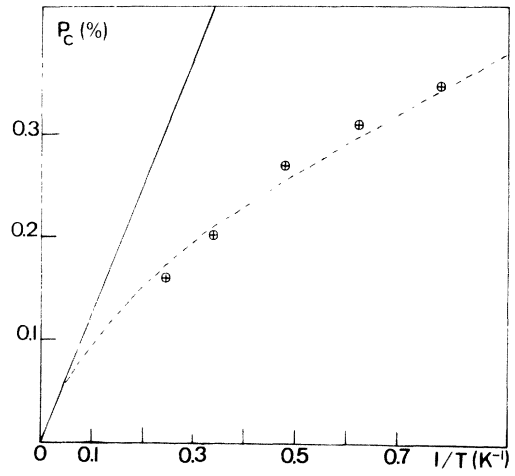

FIG. 3. Temperature-dependent terms of P_C; $H = 0.85$ T. The solid line corresponds to zero internal stress. The dashed curve corresponds to 4 kg·mm^{-2} internal stresses. Crossed circles correspond to experimental points.

We therefore expect P_C to be 3.7 and 13.3% at 4.2 and 1.2K, respectively.

Figure 2 shows the experimental spectrum of P_C measured for a 0.85 T magnetic field. We have plotted on Fig. 3 the variation of P_C versus the temperature. It clearly appears that the experimental value of P_C is much smaller than the expected one.

In order to explain this quenching, we have to analyze more carefully the various perturbations which may lift the degeneracy of the $^1T_{2g}$ level and take into account the way in which the system thermalizes.

Before the magnetic field is applied, the level is actually split by *random internal stresses*. We have observed through our stress experiments that the trigonal splitting of the $^1T_{2g}$ level is at least an order of magnitude smaller than the tetragonal one. We shall therefore calculate only the contribution of the tetragonal internal stresses. We assume a statistical repartition of these stresses with a given half-width, whose order of magnitude has been evaluated through the half-width of the zero-phonon line associated with the transition $^3A_{2g} \rightarrow {}^3T_{2g}$ (T_2). For the sample used in our magnetic experiments, it was found to be 5 cm^{-1}.

When a magnetic field is applied along the [001] axis on a crystal where tetragonal internal stresses are present, two relaxation processes can be distinguished. The first one occurs between sublevels which are split by the internal stresses; this process is analyzed in Sec. V, and we are thus able to take it into account. The second process is predominant between the sublevels whose wave functions are mainly $|{}^1T_{2g}, +1\rangle$ and $|{}^1T_{2g}, -1\rangle$. Con-

siderations which are developed in Sec. VI lead to an estimation of its efficiency.

From the values of the internal stresses and the relaxation times, we have computed (in the temperature range 1.2–4.2 K) the degree of circular polarization associated with various Zeeman matrix elements in order to take into account a possible Jahn-Teller quenching. By fitting the experimental and calculated values of P_C, we found that the Zeeman matrix element is indeed reduced, the reducing factor being

$$Q = 0.08 \ .$$

It should be noted that the P_C measurements, though very sensitive, are not very precise, particularly because of stray signals due to the optical quality of the samples, or to the optics. This introduces an error estimated at 30%.

The quenching factor being expressed as

$$Q = \exp\left(-\frac{3}{2}\sum_i \frac{(E_{JT})_i}{\hbar\omega_i}\right) ,$$

we calculated the Jahn-Teller energy assuming an equal coupling to the E_g modes, whose Green's function is given in Ref. 3 as

$$E_{JT} = 515 \pm 60 \text{ cm}^{-1} \ .$$

B. Comparison with moment data

As suggested to us by Ham, it is possible to get a maximum value for the Jahn-Teller energy through the second-order moment of the fluorescence spectrum.

This spectrum may be represented as the convolution of two *shape functions* $g(E)$ and $h(E)$, $g(E)$ giving the distribution of odd-parity modes which make the transition allowed through one-phonon processes, and $h(E)$ representing the broadening due to even-parity modes. This line shape is then

$$F(E) = \int_{-\infty}^{+\infty} g(E')h(E - E')\,dE' \ .$$

We define the zeroth-, first-, and second-order moments of $F(E)$ as

$$\langle E^0\rangle_F = \int_{-\infty}^{+\infty} F(E)\,dE \ ,$$

$$\langle E^1\rangle_F = \bar{E} = \int_{-\infty}^{+\infty} EF(E)\,dE \ ,$$

$$\langle E^2\rangle_F = \int_{-\infty}^{+\infty} (E - \bar{E})^2 F(E)\,dE \ ;$$

For $g(E)$ and $h(E)$ the definitions are similar.

One can then prove that

$$\langle E^2\rangle_F = \langle E^2\rangle_g + \langle E^2\rangle_h = \langle E^2\rangle_g + \langle E^2\rangle_{A_{1g}} + \langle E^2\rangle_{E_g} + \langle E^2\rangle_{T_{2g}} \ .$$

$\langle E^2\rangle_g$ can be estimated from Manson's T_{1U} Green's function, and $\langle E^2\rangle_F$ can be calculated from the experimental fluorescence spectrum. If we assume that the entire additional broadening is due to the E_g modes, then

$$\langle E^2\rangle_h = \langle E^2\rangle_F - \langle E^2\rangle_g = \sum_i (E_{JT})_i \hbar\omega_i \ .$$

This leads to the maximum value of the Jahn-Teller energy

$$E_{JT} \leq 555 \text{ cm}^{-1} \ .$$

In the limit where the coupling with all the E_g modes is not very different, these results show that the coupling to the A_{1g} and T_{2g} modes is actually weak.

V. RELAXATION PROCESSES

In the specific state we are studying, the Jahn-Teller coupling quenches the operator which induces the relaxation between the sublevels split by a [001] stress; therefore it makes the relaxation time longer. In the temperature range in which we are working, this relaxation time happens to have the same order of magnitude as the fluorescence lifetime.

A. Tunneling process

In this Jahn-Teller configuration, the ground-state vibronic wave functions are fairly well localized. Moreover, when only coupling with E_g modes is considered, the electronic wave functions of the triplet remain mutually orthogonal. This should lead, at low temperature (when $kT \ll E_{JT}$), to a static Jahn-Teller effect; there should be no transfer from one potential well to another.

When a [001] stress is applied, the relative energies of the potential wells are changed. However, since the splitting remains very small compared to the Jahn-Teller energy, the fluorescence spectrum, in the absence of relaxation, should not be polarized.

We observed a large degree of P_L, meaning that some relaxation occurs through a quantum process between the potential wells, leading to unequally populated vibronic states.

B. Study of dynamic processes through static P_L experiments

The relaxation processes may be studied through the temperature and stress dependence of P_L. In order to calculate it, the following hypothesis are required: (i) The sublevels of the relaxed excited state are equally populated by pumping and fast relaxation processes (we use natural excitation light). (ii) The influence of random internal tetragonal stresses is negligible (in the sample we used in stress experiments, their half-width is 0.5 Kg mm^{-2}). (iii) The fluorescence lifetime T_F does not depend upon the stress; the $^1T_{2g}$ level is fairly well isolated from the levels that could be mixed with it

by the [001] stress. Nor does τ_F depend upon the temperature; we measured it at various temperatures and found it to be 0.7×10^{-5} sec.

The relaxation time τ_R is analogous to the reorientation time for paraelastic systems.[10,11]

The stress is applied along the [001] axis. The emission light is then mostly polarized parallel to the stress; from the selection rules, we may conclude that the $|{}^1T_{2g}, XY\rangle$ singlet is lower than the $|{}^1T_{2g}, YZ\rangle$, $|{}^1T_{2g}, XZ\rangle$ doublet energy.

Under these conditions, the equations of the pumping cycle are

$$\frac{dN_{XY}}{dt} = \lambda - \frac{N_{XY}}{\tau_F} - \frac{N_{XY}}{\tau_R} + \frac{(N_{XY}+N_{YZ}+N_{XZ})e^{X}}{\tau_R(e^{X}+2e^{-X})} ,$$

$$\frac{dN_{YZ}}{dt} = \frac{dN_{XZ}}{dt} = \lambda - \frac{N_{YZ}}{\tau_F} - \frac{N_{YZ}}{\tau_R} + \frac{(N_{XY}+N_{YZ}+N_{XZ})e^{-X}}{\tau_R(e^{X}+2e^{-X})} .$$

N_{XY}, N_{YZ}, and N_{XZ} are the populations of the $|{}^1T_{2g}, XY\rangle$, $|{}^1T_{2g}, YZ\rangle$, and $|{}^1T_{2g}, XZ\rangle$[2] states, respectively; λ is the pumping rate; $X=\Delta E/2kT$, where ΔE is the splitting induced by the stress.

The above expressions lead to the formula for P_L under stress:

$$P_{L\,001} = [\tfrac{3}{8}f(X)]\,[1+\tau_R/\tau_F+\tfrac{1}{8}f(X)]^{-1}, \qquad (1)$$

where $f(X)=(e^{X}-e^{-X})/(e^{X}+2e^{-X})$.

Equation (1) shows that it is possible to identify τ_R through the temperature and stress dependence of P_L.

C. Evidence for a one-phonon-assisted tunneling process

1. Temperature dependence

If we suppose that, for weak values of X, the τ_R dependence on stress may be neglected,[12,13] we can study the temperature dependence of τ_R by deriving the slope at the origin from our experimental curve (Fig. 4). According to Eq. (1), the slope Y at the origin is proportional to

$$(1/T)(1+\tau_R/\tau_F)^{-1} . \qquad (2)$$

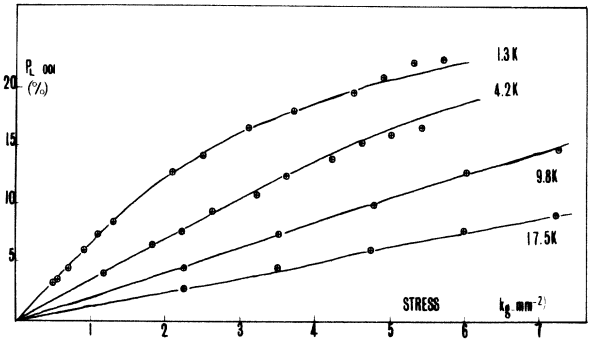

FIG. 4. $P_{L\,001}$ versus stress at various temperatures. The solid curves have been theoretically derived from experimental parameters.

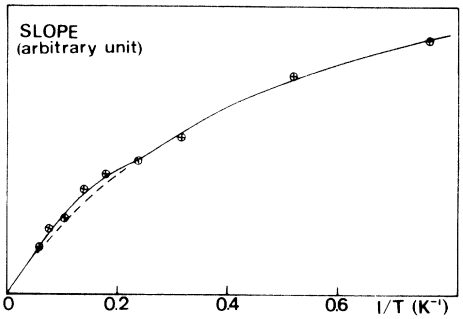

FIG. 5. Slope Y at the origin of the $P_{L\,001}$ curves versus T^{-1}. Crossed circles correspond to experimental points. The solid curve is deduced from the experimental data. The dashed curve is an hyperbola corresponding to a one-phonon direct process.

With the help of Eq. (2), and of our experimental results (Fig. 5), two processes may be distinguished, according to the formula

$$\tau_R^{-1} = 0.77\times10^{5}\,T + 40\,T^{5} .$$

One process is associated with a T^{-1} law and is predominant at low temperatures. It is interpreted as a one-phonon-assisted tunneling process, which was already observed for the reorientation time of O_2^- in alkali halide crystals[12] and in Jahn-Teller systems.[14]

Multiphonon processes usually become predominant at intermediate temperatures. Our experimental results are consistent with a T^{-5} law, i.e., with a two-phonon process.[12,14] Nevertheless, because of the experimental error, $\tau_R^{-1}=40T^{5}$ must be considered as an order of magnitude only.

2. Stress dependence

The stress dependence of τ_R is worthy of study below 4.2K, when X reaches large values. For weak values of X, we may define $\tau_R(0)$, which is the limit of τ_R when X approaches zero. For large values of X we have

$$\tau_R(X,T) = \tau_R(0,T)/\phi(X) .$$

By replacing τ_R by $\tau_R(X,T)$ in Eq. (1), we have derived $\phi(X)$. The experimental values of $\phi(X)$ at 1.3 and 4.2K are plotted in Fig. 6.

The stress dependence of a one-phonon-assisted tunneling process is the same as in the case of O_2^-.[12] The calculation leads to

$$\phi(X) = 2X(e^{2X}+2)/3(e^{2X}-1) .$$

The agreement between the theoretical curve and the experimental points confirms the nature of the relaxation process below 4.2K as a one-phonon-assisted tunneling process.

Finally, in Fig. 4, we show the theoretical variation of $P_{L\,001}$ versus stress at 1.3, 4.2, 9.8, and

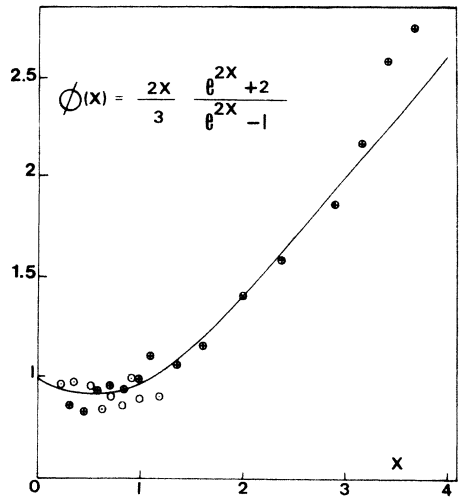

FIG. 6. Stress dependence of the relaxation time: $\phi(X) = \tau(0)/\tau_R(X)$ vs $X = \Delta E/2kT$ (see text). Crossed and dotted circles correspond to experimental points at 1.3 and 4.2 K, respectively.

17.5 K, using the experimental parameters previously determined. The general agreement is quite good, since our experimental $P_{L\,001}$ values differ by less than 5% from the theoretical ones.

VI. DISCUSSION

A. Relaxation in the presence of a uniaxial stress

The existence of a tunneling process implies that the three orthogonal wave functions $|{}^1T_{2g}, XY\rangle$, $|{}^1T_{2g}, XZ\rangle$, and $|{}^1T_{2g}, YZ\rangle$ are mixed by a trigonal operator in order to make the overlap integral nonzero. A calculation similar to that of Ref. 12, but performed in the case of a threefold degeneracy, leads to the tunneling matrix element Γ, which appears explicitly in the transition probability of the relaxation processes, and may be calculated from the experimental data.

We found $\Gamma = 3.10^{-2}\,\mathrm{cm}^{-1}$, a value quite consistent with the fact that it is considered to be a small perturbation.

Among the different processes which may cause the mixing of the wave functions, the trigonal random internal stresses have to be considered. As will be shown in the Appendix, a Gaussian distribution of internal stresses leads to a variation of the relaxation time versus temperature which is inconsistent with our experimental results. In addition, we have obtained similar results using samples where internal stresses were quite different. The internal stresses must therefore be ruled out as physical origins for the tunneling process.

It is presently impossible to experimentally check the existence of any other trigonal perturbation.

B. Relaxation in the presence of a magnetic field

As was already pointed out in Sec. IV, two processes may be efficient when a magnetic field is applied in the presence of random internal stresses. The one-phonon-assisted tunneling process, which occurs between levels whose wave functions are localized by a tetragonal stress, has been studied in Sec. V.

The relaxation processes which occur between the $|{}^1T_{2g}, +1\rangle$ and $|{}^1T_{2g}, -1\rangle$ states are not known experimentally. The Jahn-Teller energy would be 560 cm^{-1} if these two states were completely thermalized, and 370 cm^{-1} if they were equally populated.

Actually, we are able to obtain a better estimate of the Jahn-Teller energy if we assume a one-phonon direct process between the states $|{}^1T_{2g}, +1\rangle$ and $|{}^1T_{2g}, -1\rangle$. This is quite reasonable, since we operate at very low temperatures.

We can theoretically compare the relaxation times associated with a one-phonon-assisted tunneling process, and with a one-phonon direct process (τ_1 and τ_2, respectively). Symmetry considerations show that the former process may be induced by A_{1g} or E_g phonons; the latter process by E_g or T_{2g} phonons.

In order to estimate the ratio τ_2/τ_1, we will only consider the relaxation induced by E_g phonons. The coupling with T_{2g} phonons may actually be neglected, because the associated matrix element is quenched by the Ham factor. Coupling coefficients are not known for A_{1g} phonons.

The derivation of τ_2/τ_1 requires the usual expression of τ_2 as a function of the splitting $2\delta E$, and the expression previously cited from Ref. 12 as a function of the tunneling matrix element Γ in the case of τ_1.

In the limit of weak values of the stress [$\phi(X) \sim 1$], and of the magnetic splitting $2\delta E$ ($2\delta E \ll kT$), this ratio is

$$\tau_2/\tau_1 = (\Gamma/2\delta E)^2 .$$

From τ_2/τ_1, we can deduce the ratio τ_2/τ_F and take it into account in order to calculate the thermalization and the Ham factor. This has been done in Sec. IV.

VII. CONCLUSION

The study of magnetically and stress-induced polarization of the fluorescence spectrum of the ${}^1T_{2g}$ relaxed excited state has shown a major interaction with the E_g modes, leading to a Jahn-Teller energy of about 515 cm^{-1}. The influence of random internal stresses has been taken into account in order to get quantitative results. Furthermore, these static experiments allowed us to analyze the relaxation processes in the range 1.2–17 K; a one-phonon-

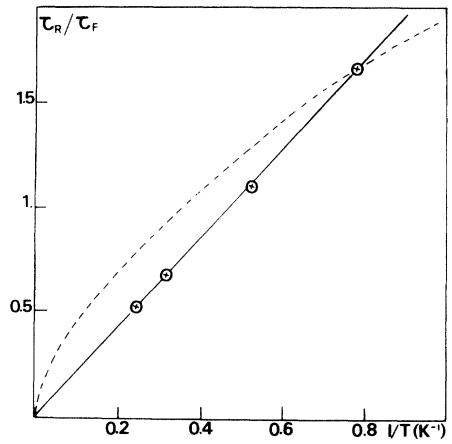

FIG. 7. τ_R/τ_F vs T^{-1}. The solid line corresponds to a fixed value of γ, crossed circles correspond to experimental points. The dashed line is associated to a random distribution of γ; the fit is on the point at 1.3 K (see text).

assisted tunneling process has been identified through its stress dependence. However, its physical origin is not yet known.

Such experimental studies, which provide information about relaxed excited states of ions in crystals, also extend the field of investigation of tunneling processes in solids.

ACKNOWLEDGMENTS

We are grateful to Y. Merle d'Aubigné for fruitful remarks, and to F. S. Ham and R. H. Silsbee for illuminating discussions. We thank P. J. Stephens, Y. Farge, and M. Regis for supplying us with samples.

APPENDIX

The following calculation is performed under the assumption of a one-phonon direct process. When only one relaxation time is considered, the P_L experiments, as was previously shown [in Eq. (1)], lead to the T^{-1} variation of τ_R. If the relaxation is induced by random internal stresses, a random distribution of relaxation times must be considered; this leads to a more complicated formula for the P_L

$$P_{L\,001} = \frac{1}{\sqrt{\pi}\,\gamma_0} \int_{-\infty}^{+\infty} e^{-\gamma^2/\gamma_0^2} \times \left(\tfrac{3}{8} f(X)\right)\left(1 + \tau_R/\tau_F + \tfrac{1}{8} f(X)\right)^{-1} ,$$

where γ is the random value of the stress, γ_0 is the half-width of the distribution, and $\tau_R = K/T\,\phi(X)$, K being a constant factor. $\phi(X)$ has been defined in Sec. V C 2.

By identifying the experimental value of P_L for a given temperature with the theoretical value, we compute the half-width γ_0 which would induce this value of the P_L. We then calculate the variation of the P_L versus temperature that would be expected for this specific distribution of internal stresses. We can finally deduce the relaxation time that could be measured with the method described in Sec. V. The variation of this time is shown on Fig. 7.

---

*Equipe de recherche $n°$ 5 du Centre National de la Recherche Scientifique.

[1]M. D. Sturge, Solid State Phys. 20, 91 (1967).
[2]J. Duran, Y. Merle D'Aubigné, and R. Romestain, J. Phys. C 5, 2225 (1972).
[3]N. B. Manson, Phys. Rev. B 4, 2656 (1971).
[4]B. D. Bird, G. A. Osborne, and P. J. Stephens, Phys. Rev. B 5, 1800 (1972).
[5]M. Billardon, J. C. Rivoal, and J. Badoz, Rev. Phys. Appl. 4, 353 (1969).
[6]M. J. Harding, S. F. Mason, D. J. Robbins, and A. J. Thomson, J. Chem. Soc. A 3047 (1971).
[7]D. J. Robbins, Ph. D. thesis (University of East Anglia, 1971) (unpublished).
[8]F. S. Ham, Phys. Rev. 138, 1727 (1965).
[9]M. J. Harding (private communication).
[10]W. Kanzig, J. Phys. Chem. Solids 23, 479 (1962).
[11]V. Narayanamurti and R. O. Pohl, Rev. Mod. Phys. 42, 201 (1970).
[12]R. Pirc, B. Zeks, and P. Gosar, J. Phys. Chem. Solids 27, 1219 (1966).
[13]R. H. Silsbee, J. Phys. Chem. Solids Suppl. 28, 2525 (1967).
[14]F. I. B. Williams, D. C. Krupka, and D. P. Breen, Phys. Rev. 179, 255 (1969).